

# Constraints on $\Delta G$ from Prompt Photon plus Jet Production at HERA- $\vec{N}$

L. E. Gordon

*High Energy Physics Division, Argonne National Laboratory, Argonne, IL 60439*

## Abstract

The utility of prompt photon plus associated jet production for constraining the size and shape of the polarized gluon density of the proton  $\Delta G$  is examined at  $\sqrt{S} = 40$  GeV, appropriate for the proposed HERA- $\vec{N}$  polarized  $\vec{p}\vec{p}$  collider experiment. The calculation is performed at next-to-leading order ( $O(\alpha_s^2)$ ) in QCD. The reliability of the predictions are examined in some detail.

## I.

Polarized deep inelastic scattering (DIS) experiments have proved invaluable for providing information on the spin-dependent parton densities of the nucleon [1–3] through measurement of the polarized structure functions such as  $g_1^p(x, Q^2)$ . Data from such experiments have traditionally been used in phenomenological analyses which attempt to constrain the polarized parton densities and evolve them in  $Q^2$  through the use of the spin-dependent Altarelli-Parisi evolution equations. Up until fairly recently, all such analyses had to be performed in leading order (LO) QCD since the spin-dependent two loop splitting functions were unknown. Since the two-loop splitting functions have been calculated [4,5], recent analyses have been performed in next-to-leading order (NLO) QCD [6–8] and parametrizations of the polarized parton densities have been provided which can be used in calculations of other polarized processes.

In these analyses extensive use is made of theoretical constraints such as the Bjorken sum rule in order to extract the parton densities from the polarized structure function measurements. Despite this the data does not provide tight constraints on sizes, and even more so the shapes of either the polarized quark ( $\Delta q$ ) or gluon ( $\Delta G$ ) densities. This is true in particular for  $\Delta G$ . Each group provides more than one different parametrization of the parton densities, each set fitting the structure function data, but they can have very different individual parton densities reflecting the limited constraints on these quantities provided by DIS experiments. It is thus very important, if our understanding of the spin structure of the nucleon is to be improved, that accurate measurements of these distributions be obtained from other processes.

Since the cross section for prompt photon production is dominated by the subprocess  $qg \rightarrow \gamma q$  in hadronic collisions already in leading order, it has proved very useful for providing information on the unpolarized gluon densities,  $g(x, Q^2)$ , of hadrons at fixed target facilities. It has therefore been suggested that it may prove equally useful in pinning down the polarized gluon densities [9]. In this context it has been examined quite extensively.

The NLO corrections were calculated in [10] and [11], where numerical estimates were also presented and it was established that the LO results were perturbatively stable. In both those analyses only LO polarized parton densities were available and the fragmentation contributions were not included. More recently, prompt photon production with polarized beam and target was examined in ref. [12,13] using NLO polarized parton densities and including the fragmentation contributions.

Although single inclusive prompt photon production will definitely be very important for constraining the size of  $\Delta G$ , information on the detailed  $x$ -shape of the distribution may not be as easily extracted. This is because the calculation of the inclusive cross section involves one convolution over the momentum fractions,  $x$ , of the initial partons. The practical effect of this is that a measurement of the kinematic variables of the photon is not sufficient to determine the value of  $x$ . If, on the other hand, one or more of the jets produced in the reaction is also tagged, no convolution is involved in the calculation and the cross section is directly proportional to the parton densities. Thus the double longitudinal asymmetry  $A_{LL}$  is directly proportional to the ratio  $\Delta G/g$  [14] in kinematic regions where other subprocesses such as  $q\bar{q}$  scattering can be neglected.

Schematically the cross section is given in terms of the polarized and unpolarized hard subprocess cross sections  $(\Delta)\hat{\sigma}_{ij}$  and parton densities  $(\Delta)f_i^a(x_a, M^2)$  (the presence of the  $\Delta$  before a quantity means the polarized version of the quantity) by

$$(\Delta)\sigma = \sum_{i,j} (\Delta)f_i^a(x_a, M^2) * (\Delta)f_j^b(x_b, M^2) * \left[ (\Delta)\hat{\sigma}_{ij}^{dir} + \sum_c (\Delta)\hat{\sigma}_{ij \rightarrow c}^{frag} * D_c^\gamma(z, M_F^2) \right]. \quad (1.1)$$

The  $*$  indicates either a product or convolution and explicit dependence of the hard subprocess cross sections on the kinematic variables of the observed products and the renormalization and factorization scales have been omitted. The sum over  $i, j$  extends over all initial partons and  $D_c^\gamma(z, M_F^2)$  is the unpolarized fragmentation function for a parton,  $c$ , into a photon at scale  $M_F^2$ . Thus, just as in the single photon case, there are two classes of contributions to the cross section labelled the *direct* and *fragmentation* contributions.

The polarized and unpolarized parton densities are defined by

$$\Delta f_i(x, M^2) = f_i^+(x, M^2) - f_i^-(x, M^2) \quad (1.2)$$

and

$$f_i(x, M^2) = f_i^+(x, M^2) + f_i^-(x, M^2), \quad (1.3)$$

where the  $f_i^+$  and  $f_i^-$  represent the distribution of partons of type  $i$  with positive and negative helicities respectively, with respect to that of the parent hadron. The hard subprocess cross sections are defined by

$$\Delta \hat{\sigma}_{ij} = \frac{1}{2} (\sigma^{++} - \sigma^{+-}) \quad (1.4)$$

and

$$\hat{\sigma}_{ij} = \frac{1}{2} (\sigma^{++} + \sigma^{+-}). \quad (1.5)$$

One of the main quantities studied in polarized experiments is the longitudinal asymmetry  $A_{LL}$ . This quantity gives a measure of the sensitivity of the process to polarization effects. The double spin asymmetry studied in this paper is defined by

$$A_{LL} = \frac{\Delta \sigma}{\sigma}, \quad (1.6)$$

the ratio of the cross section for longitudinal polarization of the incoming hadrons to the corresponding unpolarized cross section.

In LO the direct processes contributing to the cross section are  $qg \rightarrow \gamma q$  and  $q\bar{q} \rightarrow \gamma g$ . In a LO jet calculation, the simple approximation ‘parton = jet’ is used irrespective of the jet definition used in the experiments, hence either the final state gluon or quark will form the jet. It is only in NLO that more than one parton may make up a jet, and one finds a dependence of the cross section on the jet definition and parameters. In addition there are the fragmentation processes:

$$qg \rightarrow qg$$

$$qq \rightarrow qq$$

$$\begin{aligned}
qq' &\rightarrow qq' \\
q\bar{q} &\rightarrow q\bar{q} \\
gg &\rightarrow gg \\
q\bar{q} &\rightarrow gg \\
gg &\rightarrow gg \\
gg &\rightarrow q\bar{q}
\end{aligned} \tag{1.7}$$

where one of the final state partons fragments to produce the photon, i.e.,  $q(g) \rightarrow \gamma + X$ .

The cross section of interest here is the triple differential cross section

$$\frac{d^3\Delta\sigma^{\gamma J}}{dp_T^\gamma d\eta^\gamma d\eta^J},$$

where  $\eta^\gamma$  and  $\eta^J$  are the pseudorapidities of the photon and jet respectively and  $p_T^\gamma$  is the transverse momentum of the photon. The direct contribution to the cross section is given in LO by

$$\frac{d^3\Delta\sigma^{\gamma J}}{dp_T^\gamma d\eta^\gamma d\eta^J} = 2\pi p_T^\gamma \sum_{i,j} x_a \Delta f_i^a(x_i, M^2) x_b \Delta f_j^b(x_j, M^2) \frac{d\Delta\hat{\sigma}_{ij}}{d\hat{t}}. \tag{1.8}$$

The corresponding fragmentation contributions will involve a convolution over the fragmentation variable  $z$ .  $\hat{s} = x_a x_b S$  where  $\sqrt{S}$  is the cms energy in the hadron-hadron system and as usual,  $\hat{t} = (p_1 - p_\gamma)^2$  where  $p_1$  and  $p_\gamma$  are the momenta of one of the initial state partons and the observed final state trigger photon respectively. The Bjorken variables,  $x_{a,b}$ , are given in terms of the kinematic variables of the photon and jet by

$$\begin{aligned}
x_a &= \frac{p_T^\gamma}{\sqrt{S}} (e^{\eta^\gamma} + e^{\eta^J}) \\
x_b &= \frac{p_T^J}{\sqrt{S}} (e^{-\eta^\gamma} + e^{-\eta^J}).
\end{aligned} \tag{1.9}$$

In leading order  $p_T^\gamma = p_T^J$  and thus a measurement of  $p_T^\gamma$ ,  $\eta^\gamma$  and  $\eta^J$  means that  $x_{a,b}$  can be determined. In other words, a measurement of  $d^3\Delta\sigma^{\gamma J}/dp_T^\gamma d\eta^\gamma d\eta^J$  corresponds to a measurement of  $d^2\Delta\sigma^{\gamma J}/dx_a dx_b$ . In NLO due to the presence of a third parton in the process this simple formula is no longer applicable. In that case, in order to determine  $x_{a,b}$

unambiguously, one would need to measure the kinematic variables of all three final state partons. The values of  $x_{a,b}$  are only approximately determined by the transverse momenta and pseudorapidities of the photon and jet in this case, due to the need to implement a jet definition. If photon isolation requirements are also implemented, then the determination of  $x_{a,b}$  from the photon and jet kinematic variables would be even less precise. Such a measurement would still nevertheless yield some very useful information on the  $x$ -dependence of the polarized parton densities as will be shown.

In NLO,  $O(\alpha\alpha_s^2)$ , there are virtual corrections to the LO non-fragmentation processes, as well as the further three-body processes:

$$q + g \rightarrow q + g + \gamma \quad (1.10a)$$

$$g + g \rightarrow q + \bar{q} + \gamma \quad (1.10b)$$

$$q + \bar{q} \rightarrow g + g + \gamma \quad (1.10c)$$

$$q + q \rightarrow q + q + \gamma \quad (1.10d)$$

$$\bar{q} + q \rightarrow \bar{q} + q + \gamma \quad (1.10e)$$

$$q + \bar{q} \rightarrow q' + \bar{q}' + \gamma \quad (1.10f)$$

$$q + q' \rightarrow q' + q + \gamma \quad (1.10g)$$

The virtual corrections as well as the three-body matrix elements were calculated in ref. [11] and I use these matrix elements in this calculation.

In principle the the fragmentation processes of eq.(1.7) should now be calculated to  $O(\alpha_s^3)$  and convoluted with the NLO photon fragmentation functions whose leading behavior is  $O(\alpha/\alpha_s)$ , but the hard subprocess matrix elements are not yet available in the polarized case. Hence unless otherwise stated, in both the polarized and unpolarized cases, I include the leading order contributions to these processes only. Numerically the fragmentation processes are not significant except at extremely low  $p_T$  due to the low cms energy of the fixed target experiment as I shall show later, but for a theoretically consistent calculation they should nevertheless be included as they help to reduce uncertainties from scale dependence.

For this calculation I use the Monte Carlo method first used in [15] for the unpolarized case of the photon plus jet calculation performed here, as well as for calculations of some other important processes, to deal with the phase space integrals. In this letter I shall not give any details of the calculation except to say that the calculation was performed in the  $\overline{MS}$  scheme using the t'Hooft-Veltman (HVBM) scheme [16] to treat  $\gamma_5$ . I refer to ref. [17] for the details of the calculation. At NLO, since there are two-to-three scattering processes included in the calculation it is possible that two partons may be too close together to be resolved as two separate jets. In this case a jet definition is required. In this calculation I use the cone definition proposed at Snowmass [18], which defines a jet as hadronic energy deposited in a cone of radius  $R_J = \sqrt{(\Delta\eta)^2 + (\Delta\phi)^2}$ . At the partonic level, if one parton forms the jet then the kinematic variable of the parton is set equal to that of the jet,  $p_J = p_i$ ,  $\eta_J = \eta_i$  and  $\phi_J = \phi_i$ , and the jet is centered on the parton. If another parton falls inside the jet cone then the jet variables are the weighted averages of those of the two partons:

$$\begin{aligned} p_J &= p_1 + p_2 \\ \eta_J &= \frac{1}{p_J} (p_1 \eta_1 + p_2 \eta_2) \\ \phi_J &= \frac{1}{p_J} (p_1 \phi_1 + p_2 \phi_2) . \end{aligned} \tag{1.11}$$

All results are displayed for  $\vec{p}\vec{p}$  collisions at the center-of-mass energy  $\sqrt{s} = 40$  GeV appropriate for the proposed HERA- $\vec{N}$  experiment at DESY [14]. For the unpolarized cross section the CTEQ3M parton densities are used throughout, and the value of  $\Lambda_{\overline{MS}}$  corresponding to this distribution is also used. Use of other unpolarized parton densities at the  $x$ -values probed here do not yield significantly different results. For the polarized case the GRSV [6] and GS [7] distributions are used with the corresponding values for  $\Lambda_{\overline{MS}}$ . The authors of ref. [6] and [7] have proposed various parametrizations of the polarized parton densities differing mainly in the choice of input for the polarized gluon density  $\Delta G$ . In the case of the GRSV distributions we use the ‘valence’ set which corresponds to a fit of the available DIS data (referred to by the authors as the ‘fitted’  $\Delta G$  scenario), the large gluon fit which assumes that  $\Delta G(x, Q_0^2) = g(x, Q_0^2)$  at input (the ‘ $\Delta G = g$ ’ scenario) and the small

gluon fit which uses  $\Delta G(x, Q_0^2) = 0$  at the input scale (the ' $\Delta G = 0$ ' scenario), which in this case starts at the very low value of  $Q_0^2 = 0.34 \text{ GeV}^2$ . The latter two distributions are intended to represent extreme choices for  $\Delta G$ . These parametrizations give gluon densities which differ in their absolute sizes as well as in their  $x$ -shape. The GS parametrizations provide three fits to the data; GS A, GS B and GS C. It has been shown that the GS A and GS B distributions do not differ very much from the  $\Delta G = g$  and fitted  $\Delta G$  sets of GRSV respectively, whereas the the GS C set is widely different from any of the others. I shall present distributions using the three GRSV sets discussed above, along with the GS C set for comparison. For the fragmentation functions I use the LO asymptotic parametrization of ref. [19]. As will be shown, the choice of fragmentation functions makes very little difference to the predictions, since these processes account for only a small fraction of the cross section.

The renormalization, factorization, and fragmentation scales are set to a common value  $\mu = p_T^\gamma$  unless otherwise stated. Dependence on  $\mu$  is examined in one of the figures below. Since there are two 'particles' in the final state, the jet and the photon, both of whose transverse momenta are large, an alternative choice might be  $\mu = p_T^J$  or some function of  $p_T^\gamma$  and  $p_T^J$ . The results of the calculations show that the magnitudes of  $p_T^\gamma$  and  $p_T^J$  tend to be comparable and that dependence of the asymmetries on  $\mu$  is slight, although the individual cross sections may vary significantly with  $\mu$ . Therefore, choices of  $\mu$  different from  $\mu = p_T^\gamma$  should not produce significantly different predictions for the asymmetries. The two loop expression for  $\alpha_s(Q^2)$  is used throughout, with the number of flavors fixed at  $N_f = 4$ , although the contribution from charm was verified to be negligible at the energies considered. The value of the jet cone size is fixed at  $R_J = 0.5$  unless otherwise stated.

Fig.1a shows the triple differential cross section as a function of  $p_T^\gamma$  of the photon for the various parametrizations. The unpolarized cross section is shown for comparison. The curves were obtained by averaging over  $\Delta\eta = 1$  and  $\Delta p_T^\gamma = 1 \text{ GeV}$  and the restriction  $p_T^J \geq p_T^\gamma$  was imposed. The upper dotted curve is for the GS A parametrization, verifying that it is very similar in both shape and size to the  $\Delta G = g$  parametrization of GRSV. All the remaining parametrizations give distributions which are distinctly different in both their shapes and



sizes. If one compares these distributions with the corresponding curves for single inclusive prompt photon production [12] one finds, apart from the expected fall in the absolute size of the cross section, that the corresponding distributions differ also in their shapes. This is most obvious for the GS C parametrization which has the most distinctly different shape. Fig.1b also shows significantly larger asymmetries than the inclusive photon case for equivalent  $p_T^\gamma$ 's. Most of these differences can be traced to the fact that for the inclusive photon case, a given value of  $p_T^\gamma$  corresponds to a much less sharply defined value of  $x$  than in the photon plus jet case. In Fig.1a,b the range  $4 \leq p_T^\gamma \leq 10$  GeV corresponds to  $0.2 \leq x_{a,b} \leq 0.5$ . It was also verified that for all parametrizations, the  $qg$  scattering process accounts for more than 90% of the cross sections. Also plotted in fig.1b are the projected statistical errors in the asymmetries,  $\delta A_{LL}$ , as estimated in ref. [14] from the formula

$$\delta A_{LL} = 0.17/\sqrt{\sigma(pb)}. \quad (1.12)$$

In [14]  $\delta A_{LL}$  has been calculated by assuming an integrated luminosity of  $240 \text{ pb}^{-1}$  and beam and target polarizations of  $P_B = 0.6$  and  $P_T = 0.8$ , and including a trigger and reconstruction efficiency of 50% with no acceptance correction. Similar errors for  $\delta A_{LL}$  were estimated in [12] by integrating the unpolarized cross section over bins of sizes  $\Delta\eta = 1$  and  $\Delta p_T = 1$  GeV. We use the same procedure here. The results indicate that for  $p_T \leq 7 - 8$  GeV the asymmetries will be distinguishable.

Fig.1c and Fig.1d are similar to Figs.1a,b but in this case both the jet and photon are restricted to the forward rapidity regions.  $\eta^\gamma$  and  $\eta^J$  are centered at +1, with  $\Delta\eta = 0.2$ . At  $p_T^\gamma = 5$  GeV this corresponds to probing  $x_{a,b}$  in bins centered at the points  $x_{a,b} = 0.07$  and  $x_{b,a} = 0.55$ . The asymmetries are smaller than in fig.1b but again there are clear distinctions in sizes and shapes for the different parametrizations.

In Fig.2 we look at distributions in  $\eta^\gamma$  at  $p_T^\gamma = 5$  GeV and allow  $p_T^J$  to vary between 5 and 20 GeV. In Fig.2a the jet is restricted to be in the central region,  $-0.5 \leq \eta^J \leq 0.5$ , and in Fig.2c it is restricted to the forward region,  $0.5 \leq \eta^J \leq 1.5$ . The asymmetry plots of Fig.2b shows important differences between the various parametrizations but that of Fig.2d

is very striking. The asymmetries are rather flat, although showing differences in shape for the various parametrizations in the positive rapidity regions, but are very large and increase very sharply in the negative rapidity region, almost approaching 1 at the edge of phase space for the  $\Delta G = g$  scenario.

An examination of Fig.2c shows that this effect originates with the difference in shapes between the polarized and the unpolarized rapidity distributions. It was argued in ref. [20] that positive rapidity correlations at collider energies are an inherent property of the hard subprocess matrix elements. Thus if one restricts the jet to be at positive rapidity then the rapidity distribution of the photon would be expected to peak in the positive rapidity region. This was verified recently in ref. [21] where prompt photon plus charm quark correlations were studied at NLO. Clearly in Fig.2c this expectation is confirmed for the unpolarized cross section, but in contrast the polarized cross sections show *negative* correlations. Since the propagators in the hard subprocess matrix elements are the same this can only be due to the differences between the polarized and unpolarized parton densities. This fact was verified by using artificial polarized parton densities of exactly the same shape as the unpolarized ones along with the polarized matrix elements. In that case positive rapidity correlations between the photon and the jet were obtained.

In ref. [20] it is suggested that it is the behavior at small- $x_a, x_b$  of the product  $x_a x_b f^a(x_a, Q^2) f^b(x_b, Q^2)$  along with the structure of the hard subprocess matrix elements which generate the positive rapidity correlations between two final state particles. It is well established that the small- $x$  behavior of the ratio  $\Delta G/g$  is  $\sim x$  as  $x \rightarrow 0$ . Hence there is an additional power of  $x$  in the polarized parton distributions at small- $x$ . This also applies in the set for which  $\Delta G = g$  at the input scale. At the scale we are considering ( $Q^2 \sim 25 \text{ GeV}^2$ ) the evolution equations determine the shape of the parton densities regardless of the shape at the input scale. Therefore given the fact that the behavior of the ratio  $\Delta G/g$  at small- $x$  is generated by the polarized Altarelli-Parisi equations themselves [9] and that the GRSV input scale is so low ( $Q_0^2 = 0.34 \text{ GeV}^2$ ), it is understandable that even the  $\Delta G = g$  scenario will also show the same small- $x$  behavior characteristic of the polarized parton densities. It

is easy to show from eq.(1.9) [20] that when only two final state particles are present, as is the case in LO

$$x_a x_b = \frac{2(p_T^\gamma)^2}{S}(1 + \cosh(\eta^\gamma - \eta^J)). \quad (1.13)$$

The effect of this additional factor is to suppress the polarized rapidity distributions at the point  $\eta^\gamma = \eta^J$  and produce two symmetrical peaks on both sides of this point. There are many other factors such as, for example, available phase space which also affect the rapidity correlations and may tend to obscure the effect of the small- $x$  behavior, but from Fig.2d the effect is a significant rise in the predicted asymmetries at negative rapidities. This strong sensitivity to polarization effects in this region should serve as a very good test of the underlying QCD mechanism as well as a check on assumptions about the small- $x$  behavior of the polarized parton densities.

In order to test the sensitivity of the predictions to the choice of factorization and renormalization scales, Fig.3a shows predictions for the asymmetry of a sample of the  $p_T^\gamma$  distributions of Fig.1a for three different scales. All hard scales are kept equal and varied simultaneously. Although, as in the case of single prompt photon production, varying the scales over the full range shown can change the individual cross sections by up to 50%, the predicted asymmetries are relatively stable. In Fig.3b the sensitivity of the predicted asymmetries to the cone size of the jet  $R_J$  and to the inclusion of the fragmentation contributions is tested. The solid lines are again the predictions of Fig.1b. Setting  $D_{c/\gamma}(z, M_F^2) = 0$  clearly has very little effect on the asymmetries, meaning that the predictions are likely to be very similar if NLO corrections to these contributions were included. This could be expected since at this cms energy, fragmentation is less than 10% of the cross section except at the very lowest  $p_T$  values. The dotted line in Fig.3b shows the effect of setting  $R_J = 1$ . The effect on the cross sections is generally less than 10% and clearly it has no effect at all on the asymmetries.

Since in this calculation a jet definition is involved in NLO, the calculation of a so-called K-factor to estimate the size of the NLO corrections is not meaningful, as it would depend

on the value of  $R_J$  chosen. Thus in Fig.3c, a comparison is made between predictions for the cross section using the LO and NLO matrix elements but both using the NLO structure functions. The aim is to examine whether the NLO matrix elements and jet definition have any effect on the shapes of the distributions. As stated earlier, in NLO, measuring the kinematic variables of the photon and jet does not serve to uniquely determine the values of  $x_a$  and  $x_b$ . Any significant differences between the values of these variables probed in LO and NLO could possibly show up as a difference in the shapes of the distributions. Figs.3a,b clearly show that there are no significant shape differences between the LO and NLO distributions, and therefore one can assume that estimating the values of  $x$  probed for a given kinematical configuration of the photon and jet by the LO formula may not lead to unacceptably large errors.

In conclusion, I have examined the possibility that both the size and  $x$ -shape of the polarized gluon distribution of the proton,  $\Delta G$ , may be measured at HERA- $\vec{N}$  via a measurement of the photon plus jet cross section. Control over the kinematic variables of both the photon and jet allows a much better determination of the  $x$ -value probed when compared to inclusive prompt photon production. A comparison of the predictions obtained using different polarized parton densities show that a clear distinction between both the sizes and shapes should be possible. Assuming that the ‘fitted  $\Delta G$ ’ scenario is the most plausible distribution, then a typical value for the asymmetry,  $A_{LL}$  is 10%, but given the uncertainty in  $\Delta G$  the asymmetry could be as small as 2% or as large as 40%. The expected small- $x$  behavior of the polarized distributions lead to predictions of negative correlations between the rapidities of the photon and jet. The effect is to produce very large asymmetries, even approaching the maximum value of  $A_{LL} = 1$  in certain kinematic regions, which should make them more easily measurable in the experiments.

## II. ACKNOWLEDGMENTS

I am indebted to Ed Berger for many helpful discussions and for reading the manuscript, and to Werner Vogelsang for some helpful comments. The work at Argonne National Laboratory was supported by the US Department of Energy, Division of High Energy Physics, Contract number W-31-109-ENG-38.

## REFERENCES

- [1] EMC, J. Ashman *et al.*, Phys. Lett. **B 206**, 364 (1988); Nucl. Phys. **B328**, 1 (1989).
- [2] SMC, B. Adeva *et al.*, Phys. Lett. **B 302**, 533 (1993). SMC, D. Adams *et al.*, Phys. Lett. **B329**, 399 (1994); **B339**, 332(E) (1994); SMC, D. Adams *et al.*, Phys. Lett. **B357**, 248 (1995).
- [3] SLAC-E142 Collaboration, P. L. Anthony *et al.*, Phys. Rev. Lett. **71**, 959 (1993); SLAC-E143 Collaboration, K. Abe *et al.*, Phys. Rev. Lett. **74**, 346 (1995); SLAC-E143 Collaboration, K. Abe *et al.*, Phys. Rev. Lett. **75**, 25 (1993).
- [4] R. Mertig and W. L. Van Neerven, Z. Phys. **C70**, 637 (1996).
- [5] W. Vogelsang, Phys. Rev. **D54** (1996) 2023; Nucl. Phys. **B475** (1996) 47.
- [6] M. Glück, E. Reya, M. Stratmann and W. Vogelsang, Phys. Rev. **D53**, 4775 (1996).
- [7] T. Gehrmann and W. J. Stirling, Phys. Rev. **D53**, 6100 (1996).
- [8] R. D. Ball, S. Forte and G. Ridolfi, Phys. Lett. **B 378**, 255 (1996).
- [9] E. L. Berger and J. Qiu Phys. Rev. **D40**, 778 (1989); **40**, 3128 (1989); S. Gupta, D. Indumathi, and M. V. N. Murthy, Z. Phys. **C 42**, 493 (1989); **44**, 356(E) (1989); H. Y. Cheng and S. N. Lai, Phys. Rev. **D 41**, 91 (1990); C. Bourrely, J. Ph. Guillet, and J. Soffer, Nucl. Phys. **B361**, 72 (1991); P. Mathews and R. Ramachandran, Z. Phys. **C 53**, 305 (1992).
- [10] A. P. Contogouris, B. Kamal, Z. Merebashvili and F. V. Tkachov, Phys. Lett. **B304** 329 (1993); Phys. Rev. **D48** 4092 (1993).
- [11] L. E. Gordon and W. Vogelsang, Phys. Rev. **D48**, 3136 (1993) and **D49**, 170 (1994).
- [12] L. E. Gordon and W. Vogelsang, ANL-HEP-PR-96-15 and RAL-TR-96-057 (hep-ph/9607442) (to be published, Phys. Lett. B).

- [13] L. E. Gordon and W. Vogelsang, Work in Progress
- [14] W.-D. Nowak "Possible Measurements of Single and Double Spin Asymmetries with HERA- $\vec{N}$ " DESY-96-095.
- [15] H. Baer, J. Ohnemus, and J. F. Owens, Phys. Lett. **B234**, 127 (1990); H. Baer, J. Ohnemus, and J. F. Owens, Phys. Rev. **D42**, 61 (1990); B. Bailey, J. Ohnemus, and J. F. Owens, Phys. Rev. **D46**, 2018 (1992).
- [16] G. t'Hooft and M. Veltman, Nucl. Phys. **B44** (1972) 189; P. Breitenlohner and D. Maison, Comm. Math. Phys. **52** (1977) 11.
- [17] L. E. Gordon, ANL-HEP-PR-96-59.
- [18] J. Huth *et. al.*, Proc. of the 1990 DPF Summer Study on High Energy Physics, Snowmass, Colorado, ed. E. L. Berger, World Scientific, 1992, p. 134.
- [19] J. F. Owens, Phys. Rev. **D26** (1982) 1600.
- [20] E. L. Berger, Phys. Rev. **D37** (1988) 1810.
- [21] B. Bailey, E. L. Berger and L. E. Gordon, Phys. Rev. **D54** (1996) 1896.

## FIGURE CAPTIONS

- [1] (a)  $p_T^\gamma$  distribution of the photon plus jet triple differential cross section  $d^3\sigma^{\gamma J}/dp_T^\gamma d\eta^\gamma d\eta^J$  for various polarized parton distributions for rapidities of the photon and jet averaged over the region  $-0.5 \leq \eta^\gamma, \eta^J \leq 0.5$ . The upper dotted curve is for the GS A polarized distributions. (b) Longitudinal asymmetries for the distributions of (a). (c) and (d) similar to (a) and (b) but for both the photon and jet rapidities averaged over the region  $0.5 \leq \eta^\gamma, \eta^J \leq 1.5$ .
- [2] (a) Distribution in the rapidity of the photon for  $p_T^\gamma = 5$  GeV and  $\eta^J$  averaged over the region  $-0.5 \leq \eta^J \leq 0.5$  and  $p_T^J \geq p_T^\gamma$ . (b) Asymmetries for the curves shown in (a). (c) and (d), similar to (a) and (b) respectively, but for  $\eta^J$  averaged over  $0.5 \leq \eta \leq 1.5$ .
- [3] (a) Scale dependence of the asymmetries shown in Fig.1b, for three parametrizations of the polarized densities. (b) Comparison of the asymmetries of Fig.1b after setting  $R_J = 1.0$  (dotted lines) and on the same plot, after neglecting the contributions from fragmentation (dashed lines). (c) Comparison of the triple differential cross section of Fig.1a with those using the LO matrix elements and (d) the corresponding asymmetries.



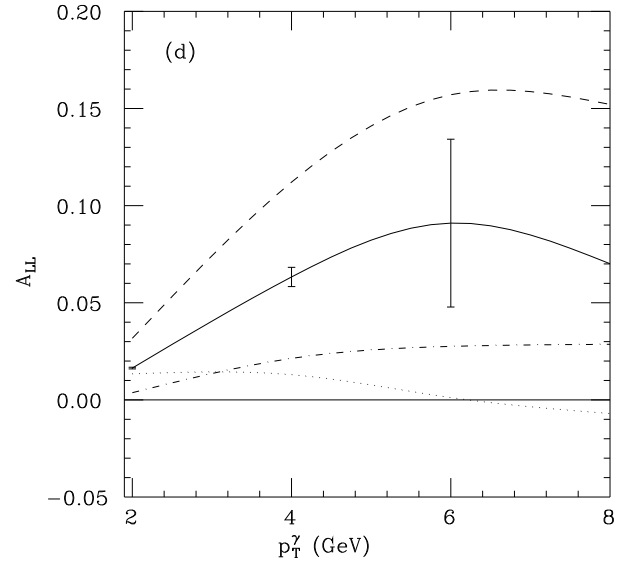
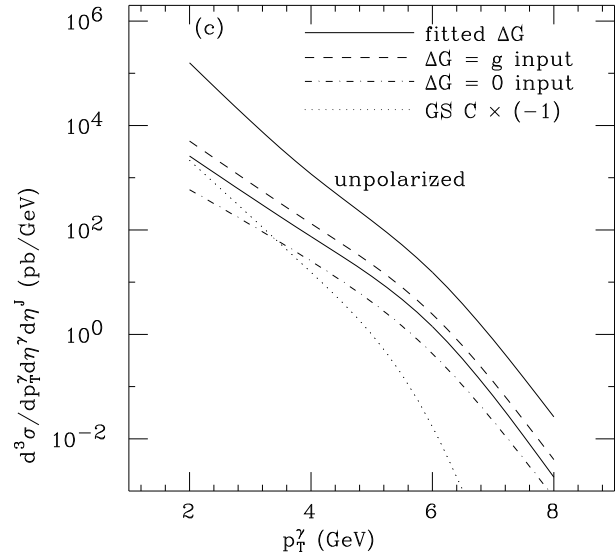
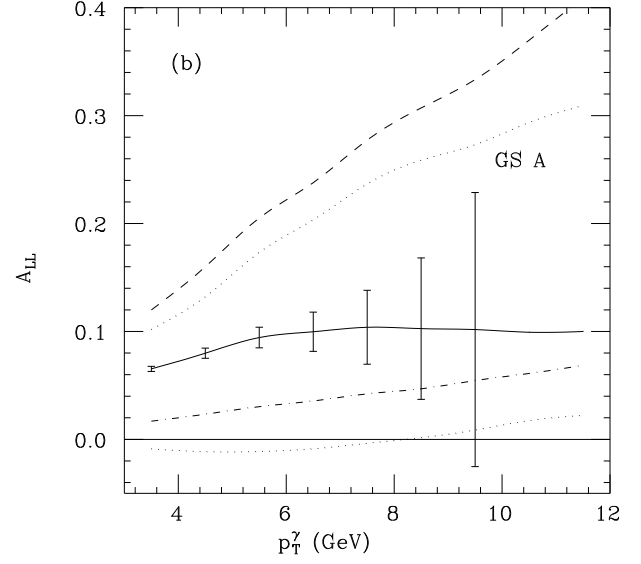
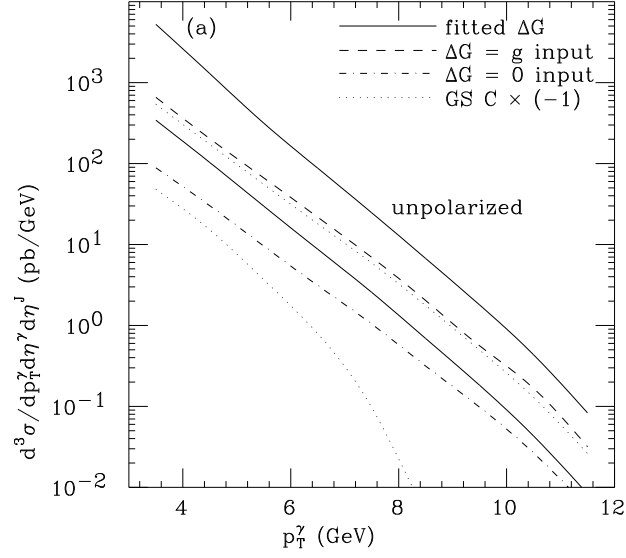


Fig. 1

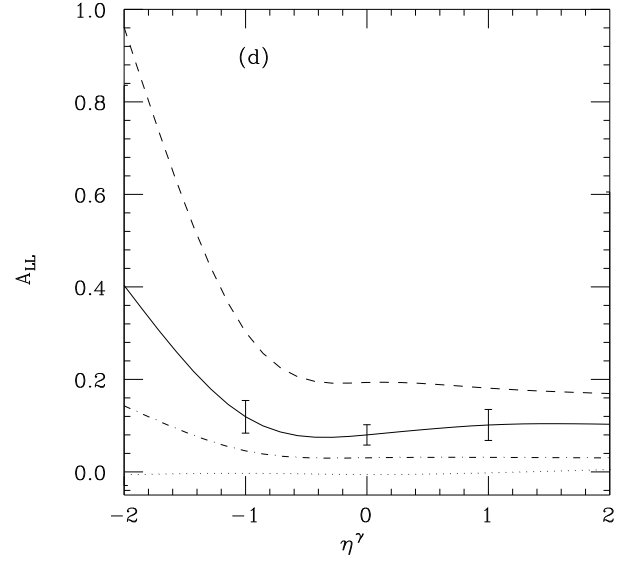
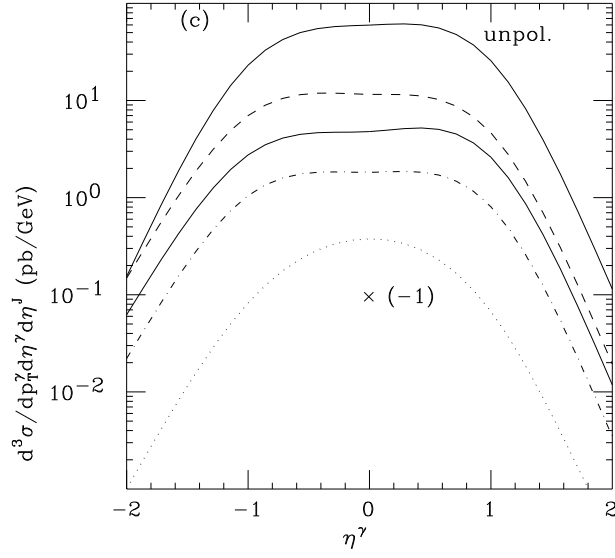
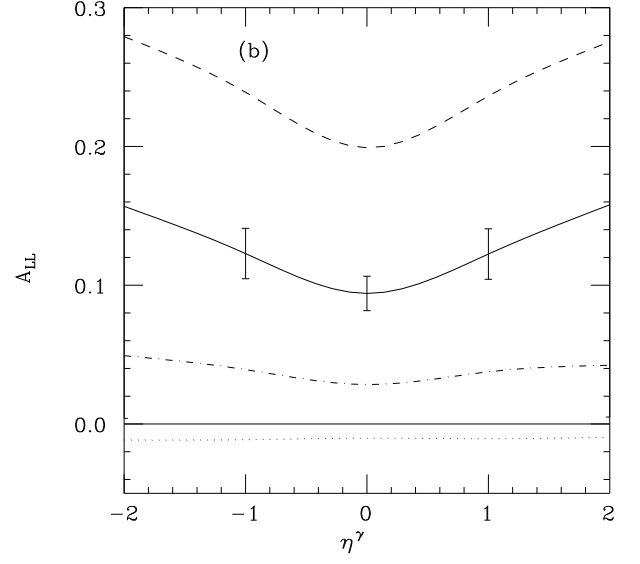
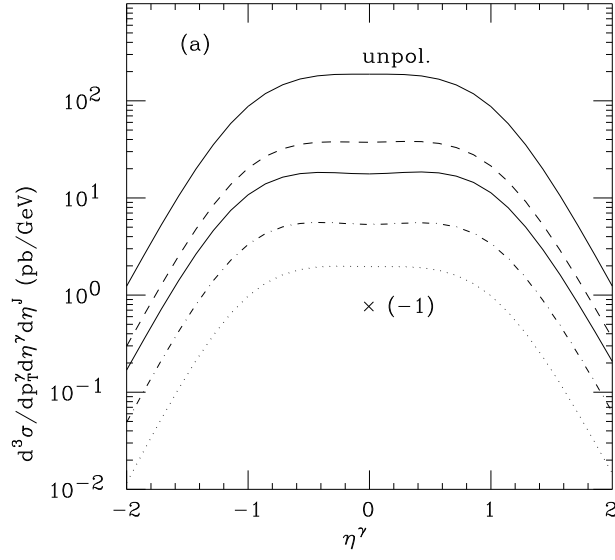


Fig. 2

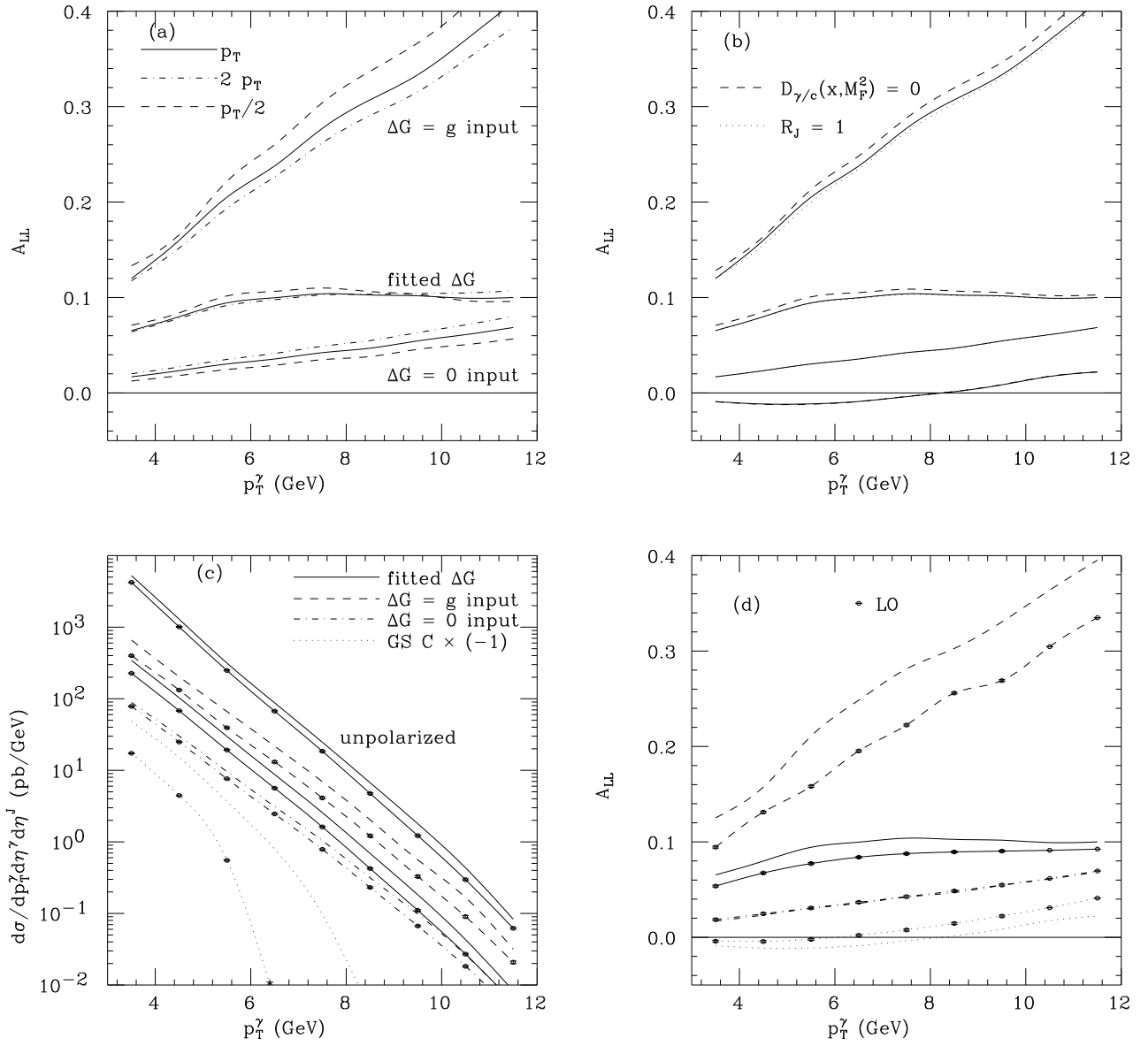


Fig. 3